MECHANICAL CHARACTERIZATION OF STRAIN-HARDENING CEMENT-BASED COMPOSITE (SHCC) UNDER DYNAMIC TENSILE LOAD

ALI. A. HERAVI[*], VIKTOR MECHTCHERINE[*]

[*]Institute of Construction Materials
Technische Universität Dresden, Germany
e-mail: ali.a.heravi@tu-dresden.de

Keywords: impact testing, split Hopkinson tension bar, fiber reinforcement, SHCC, ECC

Abstract: Strain Hardening Cement-based Composites (SHCC) (also known as ECC, Engineered Cementitious Composites) are fine-grained fiber-reinforced concretes with a very pronounced non-elastic strain capacity. SHCC exhibit a strain-hardening tensile behavior accompanied by the progressive formation of multiple controlled cracks under increasing tensile loading which results in high inelastic deformations before failure. This makes SHCC a proper material for applications where high energy absorption and damping are needed, e.g. for improving impact resistance of existing jeopardized structures.

In order to properly investigate the tensile behavior of SHCC at impact strain rates, a testing setup needs to be objectively designed based on the specific properties of the composite, namely brittle matrix, relatively large representative sample and high strain at failure (over 3% in some cases). A gravitational split Hopkinson tension bar (SHTB) was developed with the goal of investigating the dynamic tensile behavior of SHCC. The loading principle, the properties of the loading pulse and of the bar materials enable accurate characterization of the mechanical behavior of ductile cementitious composites in terms of force-deformation (stress-strain) curves under tensile impact loading. Furthermore, the design of the setup targeted several additional features, namely compact dimensions, simple operation, high adjustment flexibility and low building costs. For demonstrating the suitability of the setup the results of a normal strength SHCC tested at a strain rate of approximately 200 s^{-1} are presented and compared to the results of quasi-static tests.

1 INTRODUCTION

The relatively low tensile strength and ductility of reinforced concrete (RC) structures make them vulnerable to dynamic loading caused by earthquake, impact, or blast. An effective solution for enhancing damage tolerance and energy dissipation in existing structures is to apply thin strengthening layers made of ductile, mineral-bonded composites such as strain-hardening cement-based composites (SHCC, also known as engineered cementitious composites, ECC) [1,2]. SHCC consist of finely grained cementitious matrices and short, randomly distributed polymer micro-fibers [1,2]. These materials exhibit strain-hardening tensile behavior accompanied by the progressive formation of fine cracks under increasing tensile loading, in this way showing high inelastic deformations before failure localization and softening.

Since the complex constitutive nature of such composites results in strain rate dependent tensile ductility [3–5], mechanical investigations at the levels of composites and of individual constituents are necessary to clarify their strain-rate sensitivity and facilitate the exploitation of their full potential under high strain rates. However, the unusually high tensile ductility of these composites as compared to other types of cementitious materials requires purposefully developed testing equipment for high strain rate tests.

The split Hopkinson tension bars (SHTB) [6,7] are modifications of the original split Hopkinson pressure bar configuration developed by Kolsky [8] and represent the most common testing method for material characterization under dynamic tensile loading. The SHTBs consist of an input bar in which the loading wave is induced, a transmitter bar in which the wave transmitted by the specimen is recorded, and of a specimen which is glued between the two bars. As opposed to the Kolsky bar configuration, the SHTBs are designed for generating directly a tensile loading pulse, which is normally done by using a striker system or a pre-tensioned bar [9,10].

With the purpose of testing ductile cementitious composites with complex constitutive natures, a split Hopkinson tension bar was designed and constructed as part of a doctoral research project of the first author.

2 TESTING SETUP CHARACTERIZATION

The gravitational split Hopkinson bar is presented in **Figure 1**. The input bar (bottom) has a length of 1.36 m and the transmitter bar (top) is 2.5 m long. The transmitter bar is rigidly attached at its top end to an aluminum frame. Both bars have a diameter of 24 mm. The total height of the setup is 4.2 m, and the specimen is positioned at a height of 1.5 m. The striker device consists of two parallel, 0.4 m-long steel bars tightened to two steel blocks and positioned on both sides of the input and transmitter bars. The steel blocks are connected to each other through an aluminum plate. The distance between the parallel strikers is 60 mm, which allows their vertical motion along the entire SHTB without interfering with the instrumented bars. The 30 kg weight assembly slides down a vertical rail from a maximum drop height of 3.5 m, which ensures a 7.5 m/s impact velocity on contact with the impact flange. The impact flange is rigidly attached to the free end of the input bar at a height of 0.1 m from the base level.

Both the input and transmitter bars are instrumented with strain gauges at two distanced position along them; see **Figure 1**. At each measurement site, three strain gauges are attached to the bar axis symmetrically to prevent any error induced by possible bending moments. On the input bar two-point strain measurement is needed to find the reflected wave, and generally having two measurement points on the bars is needed to measure the accurate wave velocity.

All strain gauges are sampled with a rate of 1 MHz and are subsequently filtered with a zero-phase, 60 kHz low-pass filter in order to cancel the electrical noise and avoiding any phase shift in the signal. Data acquisition is done with the help of two synchronized SIRIUSi® HS-STG+ systems produced by DEWEsoft®.
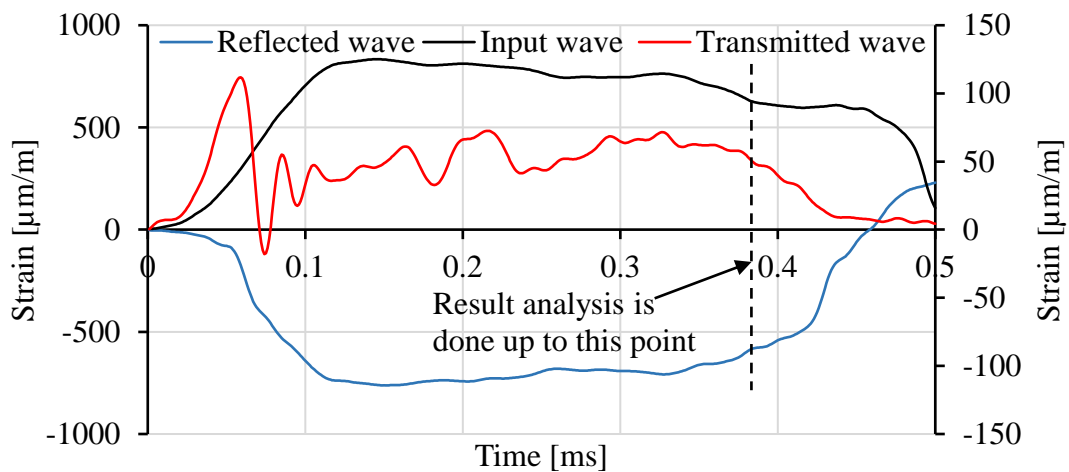
2.1 Loading principle

In order to ensure a sufficiently long input wave, the principle of rigid body motion was applied by using an impact flange made of stainless steel [11]. Owing to the high sound velocity in stainless steel and to the high structural stiffness of the flange itself, the phase of transient stress waves in the flange is considerably shorter in comparison to the total length of the loading pulse. In this way, rigid body motion of the flange occurs under the direct action of the strikers (impulse-response rigidity or force-response rigidity).

In this configuration, the length of the resulting input wave is greater than double the strikers' lengths, which allowed the use of relatively short striker**.** An example of the measured input, reflected and transmitted wave in case of an SHCC sample is presented in **Figure 2**.

The input pulse presented in **Figure 2** corresponds to a drop height of 1 m. This pulse can ensure 2.2 mm deformation in the sample at a maximum strain rate of 200 1/s. Note that a displacement of 2.2 mm is enough to achieve failure (complete separation) in 50 mm-long specimens with a strain capacity of 4 %. Such a specimen length is representative for SHCC as judged by the typical crack spacing [9] as well as for TRC specimens with textile mesh sizes of around 10 mm [12].
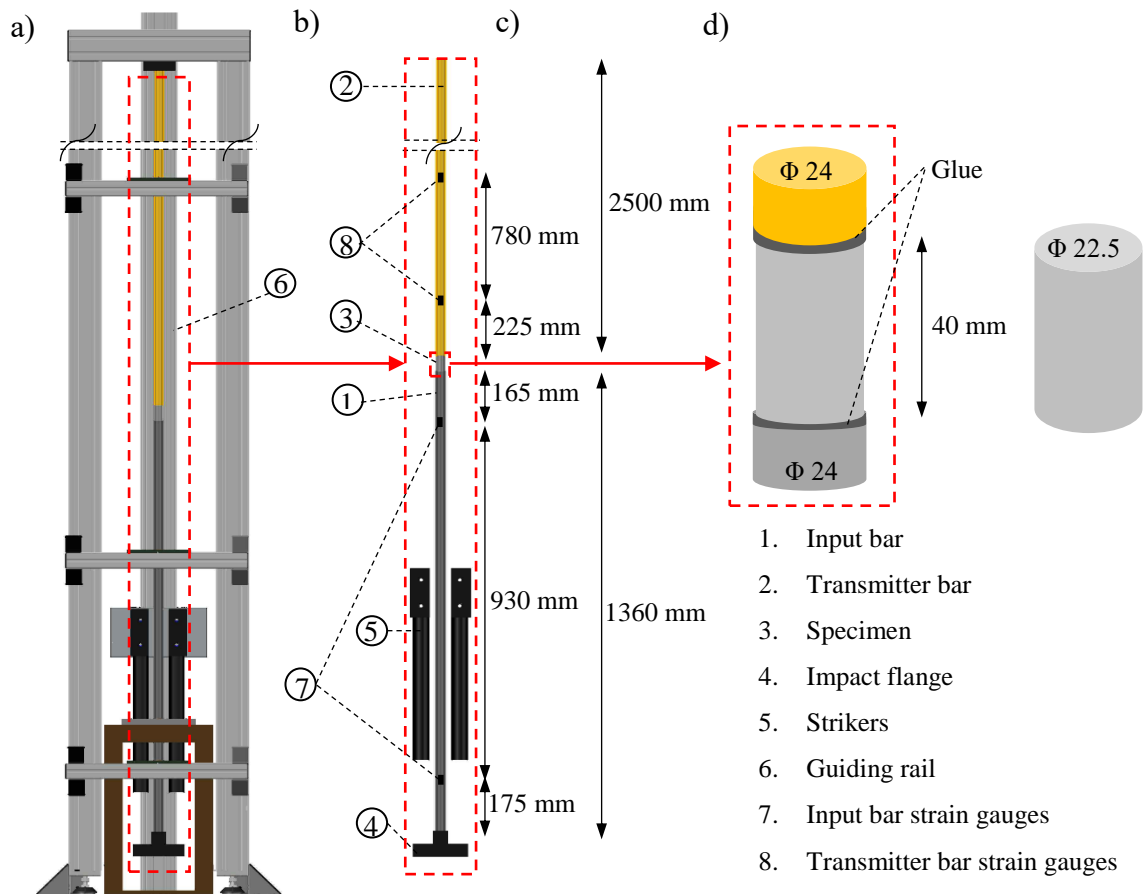
Figure 1. Gravity driven split-Hopkinson tension bar: a) schematic view of the setup, b) main components, c) position of the strain gauges and length of the bars, d) dimensions of the specimen and its attachment to the bars.

1. Input bar
2. Transmitter bar
3. Specimen
4. Impact flange
5. Strikers
6. Guiding rail
7. Input bar strain gauges
8. Transmitter bar strain gauges

Figure 2. Example of the measured input, reflected and transmitted waves; transmitted wave is shown on the secondary vertical axis.

2.2 Rise time of the loading wave and stress equilibrium

To express the material response accurately based on the wave analysis, stress equilibrium must be attained in the specimen before crack localization. Stress equilibrium is associated with a uniform stress magnitude in the specimen, and this is reached after a certain number of wave reverberations in the specimen.

3

The number of wave reverberations attained before crack initiation in cementitious materials depends on the length of the sample, on the crack formation stress, and on the wave velocity in the sample material. Since specimen length can only be reduced down to a certain limit, it is the initial phase of the loading wave, i.e. the rise time, which should be adjusted in the first place for attaining stress equilibrium prior to cracking [13].

To achieve a smooth rising phase of the loading wave, brass caps were rigidly attached to the ends of the two steel striker bars, in this way reducing the contact stiffness. Additionally, thin brass inserts were placed on the impact flange at the contact points with the striker bars. These measures ensured a rise time of the loading pulse of 0.15 ms.

Note that the required number of reverberations for reaching stress equilibrium in the sample depends also on the impedance mismatch between the sample and both input and transmitter bars [14,15]. In this study, a brass transmitter bar is used in order to increase its impedance mismatch with the sample. This can result in a faster rise of stress on upper side of the sample and reduce the time of unbalanced loading of the sample. To show the effectiveness of this measure, a series of experiments on the same material using an aluminum transmitter bar which has a lower impedance mismatch with the sample, is performed. In this experiment, the same input bar and input wave are used. The results of the experiments are presented in Section 4.2.

2.3 Wave analysis

The wave analysis is performed according to the theory of one-dimensional wave propagation [8]. The stresses at both ends of the specimen are compared for dynamic stress equilibrium, while their average is considered for the evaluation of the material properties. Eqs. 1 and 2 are used in calculating the forces at each end of the sample based on the input, reflected, and transmitted signals ($\varepsilon_I, \varepsilon_R, \varepsilon_T$). The subscripts i and t are related to the input and transmitter bars, respectively. The displacements at the ends of the sample are calculated based on Eqs. 3 and 4, where C_i and C_t are elastic wave velocities in the input and transmitter bars, respectively. The stress in the sample is calculated using Eq. 5, where A_s is the cross-sectional area of the sample. The strain in the sample is found using Eq. 6, where L_s is the length of the sample. The strain rate is calculated using the first derivative of Eq. 7 with respect to time.

$$F_i(t) = E_i A_i (\varepsilon_I(t) + \varepsilon_R(t)) \tag{1}$$

$$F_t(t) = E_t A_t \varepsilon_T(t) \tag{2}$$

$$\delta_i(t) = C_i \int_0^t (\varepsilon_I(t) - \varepsilon_R(t)) dt \tag{3}$$

$$\delta_t(t) = C_t \int_0^t \varepsilon_T(t) dt \tag{4}$$

$$\sigma(t) = \frac{F_i(t) + F_t(t)}{2 A_s} \tag{5}$$

$$\varepsilon(t) = \frac{\delta_i(t) - \delta_t(t)}{L_s} \tag{6}$$

$$\dot{\varepsilon}(t) = \frac{(\varepsilon_I(t) - \varepsilon_R(t)) C_I - \varepsilon_T(t) C_T}{L_s} \tag{7}$$

Using two measurement points on the input and transmitter bars allows deriving the elastic wave velocity and Young's modulus of the bar materials directly. The correct measurement of these parameters is of great importance in shifting the signals towards the specimens' ends as well as in deriving the stresses in the samples.

3 EXPERIMENTAL PROGRAM

3.1 Material and specimen production

The experimental series consists of quasi-static and impact tension tests on one particular SHCC material. The SHCC and its constitutive matrix were previously investigated by the authors in a pre-tensioned Hopkinson bar [4]. This investigation can serve as a reference for the current study.

The SHCC under investigation consists of a normal-strength cement-based matrix and high-performance polymer fibers as reinforcement. The normal-strength matrix M1 has a large volume of fly ash and a water-to-binder ratio of 0.3. The matrix is reinforced with 12 mm-long Ultra-High Molecular Weight Polyethylene (UHMWPE) fibers in a volume ratio of 2 %; see

Table 1. The Dyneema® UHMWPE fibers (shortly, PE) are produced by DSM, the Netherlands. Same as [4], in the paper at hand this type of SHCC is named M1-PE according to its cementitious matrix and reinforcing fiber. A detailed description of the composite and of the fiber can be found in [3,4].

Table 1. Composition of the SHCC under investigation.

M1-PE	[kg/m^3]
CEM I 42.5R-HS	505
Fly ash Steament H4	621
Quartz sand 0.06 - 0.2 mm	536
Viscosity modifying agent	4.8
Water	338
HRWRA (superplasticizer)	10
UHMWPE fiber	20

The specimen production and curing procedure were identical to those in [4]. The materials were cast in prismatic molds of dimensions 100 mm x 100 mm x 400 mm, after which cylindrical specimens were core drilled in the longitudinal direction of the beams produced. The testing age was 14 days for both loading conditions and four samples were tested for each case.

3.2 Quasi-static tension tests

The quasi-static tension tests were performed in a Zwick 1445 universal testing machine in a deformation-controlled regime with a cross-head displacement rate of 0.04 mm/s. The strain rate in the specimens before cracking was 0.001 s^{-1}.

For the quasi-static tests, 12.5 mm-thick steel rings and a special steel frame were produced for fixing the specimens in the testing machine and for attaching the Linear Variable Differential Transducers (LVDT) [4]. The steel rings were used to embed the specimens by gluing at both ends, thus ensuring non-rotatable boundary conditions. A fast hardening, bi-component glue consisting of a fluid component DEGADUR®1801 and of a powder component DEGADUR® 7742 F(N) was used.

3.3 Impact tension tests in SHTB

In the SHTB the samples were glued directly to the input and transmitter bars. For these investigations, a bi-component epoxy resin Barrafix EP produced by PCI, Germany was used as a glue. All tests are done by dropping the striker from a height of 1 m. This resulted in a speed of 4 m/s at the moment of contact with the impact flange. The strain rate of the test reached 200 s^{-1} after the first rise time of 150 µs.

4 RESULTS AND DISCUSSION

4.1 Quasi-static tension tests on SHCC

The primary mechanical parameters which define the tensile behavior of SHCC are first crack stress, tensile strength (peak tensile stress), and strain at peak tensile stress. First crack stress depends on the tensile strength of the matrix, but also on the fiber distribution, their orientation and the fiber-matrix bond properties. The hydrophobicity of the PE fibers ensures a particular mechanical interaction with the cementitious matrices, avoiding a chemical bond [16]. Furthermore, the low density and the considerable inhomogeneity of the M1 matrix further reduce the fiber-matrix bond strength.

The low fiber-matrix bond strength and the resulting weak crack-bridging capacity led to a relatively low average tensile strength of 4.5 MPa for the SHCC under investigation; see **Table 2** and **Figure 3**. The weak interfacial bond between the PE fibers and M1 matrix can also be judged by the shallow descending branches of the stress-strain curves in the softening phase, which indicate a complete fiber pullout, thus showing that the high tensile strength of the fibers is not fully exploited. A higher bond strength leading to both rupture and pull-out of the 12 mm long fibers at larger crack openings would result in a steeper softening branch.

After the formation of the first crack, the tensile stresses induced in the matrix are limited by the crack bridging capacity of the fibers. Since in the present type of SHCC, crack bridging under quasi-static loading is relatively low, cracks form only in a limited number of

cross-sections with lowest cracking stress and so leading to relatively poor multiple cracking and early localization of failure and transition into a softening regime. The moderate multiple cracking results in a low tensile strain capacity, strain up to peak tensile stress, of 1.1 %; see **Table 2**. The low tensile strength and tensile ductility also lead to a mediocre work-to-fracture of 40.3 kJ/m³. Energy is also dissipated in the softening regime; however, this is not a matter of prime interest in the current work.
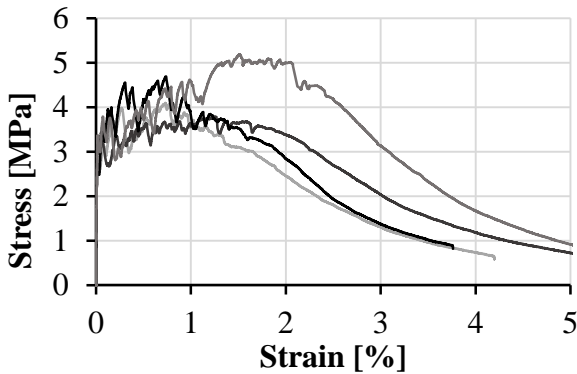
Figure 3. Quasi-static stress-strain diagrams of the SHCC under investigation.

Table 2. Quasi-static mechanical properties of M1-PE; standard deviations are given in the parentheses.

SHCC type	M1-PE
First-crack stress [MPa]	3.0 (0.4)
Tensile strength [MPa]	4.5 (0.7)
Ultimate strain [%]	1.1 (0.3)
Work-to-fracture (up to softening) [kJ/m^3]	40.3 (12.5)

4.2 Impact tension tests on SHCC

In SHCC samples as the multiple cracking starts, the equilibrium in the sample which is established before generation of the first crack is partially lost; see **Figure 4**. Depending on the position of the crack and the extent of the damage in the sample, the unloading wave created by each crack reaches the input and transmitter bar at different times. For this reason, multiple cracks introduce unsteadiness in stress values measured at two ends of the sample. Moreover, as multiple cracking occurs in the sample, the stiffness of the sample and, as a result, the wave propagation velocity

decreases significantly. This reduction in wave velocity negatively influences reestablishing the equilibrium in the sample after the first crack.

As discussed previously in **Section 2.2**, the use of the transmitter bar with higher impedance can reduce the time needed to reach equilibrium in the sample. The effectiveness of this method is shown using the tests performed on M1-PE using both aluminum and brass transmitter. The representative stress-time histories at two ends of the M1-PE sample in **Figure 4** are measured with the transmitter bar made of brass. In this figure, the first region of 100 µs is magnified to show the extent of equilibrium. **Figure 5** shows a representative stress-time history at two sides of a M1-PE sample in case of the transmitter bar made of aluminum. A comparison of the stress-time histories for M1-PE measured with two different bars as shown in **Figures 4** and **5** proves that the equilibrium in the sample is significantly improved by increasing the impedance mismatch between the sample and transmitter bars. In the case of the brass transmitter bar, the stresses at two ends of the sample equalize before peak stress. In contrast, the sample tested with aluminum transmitter bar shows deviating stresses at the two ends, and they cannot match before the peak stress related to the first crack.

The stress-strain diagrams of M1-PE presented in **Figure 6** show a peak in stress value at the beginning. This stress peak appears as a result of the strain rate sensitivity of the tensile strength in the cement-based matrices and is related to the first crack stress of the composite. The mechanisms contributing to the rate sensitivity of the matrix are: viscoelasticity of the bulk material, inertia at the crack tip, and structural level inertia. Among the mentioned sources of increase in tensile strength at high strain rate, only the first two are related to the material properties. The structural level inertia cannot be directly attributed to material performance. It depends on the geometry of the sample as well as the strain rate; moreover, it can be both in the axial and radial directions [17,18]. The influence of inertia on the results obtained should be studied in a dedicated

6

experimental program, accompanied by numerical simulations.

As the merging of micro-cracks and creation of macro-cracks continues after the peak, they cause specimen relaxation and a dramatic stress reduction. The stress drop stops as the increasing crack opening in the first macro-crack reactivates the crack bridging action of the fibers. At this moment, stress rises again, and multiple-cracking stage starts. The cracks generated at this stage appear at significantly lower stress levels. This behavior can be explained based on the fact that before the first crack a smeared damage is in progress in the matrix. As a result, the subsequent cracks appear in a partially damaged, thus weaker, matrix. Additionally, the regions between the opened cracks experience considerably lower strain rates as compared to the global strain rate. The global strain rate is considered to be the relative speed of the two ends of the sample divided by the length of the sample. At the beginning of the test and before the formation of the first macro-crack, up to 0.05 ms in **Figure 4**, the strain rate is uniform in the entire specimen length. As the first crack is formed in the sample, the strain rate in the uncracked region decreases to values close to zero. As a result, the previously discussed mechanisms responsible for the increase in tensile strength of the cement-based matrix cannot be activated to the extent to which they were in the pre-crack phase; see **Table 3**. Thus, the dynamic increase factor (DIF) of the peak crack-bridging stress (DIF = 1.7) is lower than that of the first crack stress (DIF = 4.4).

The importance of fiber-matrix bond and fibers' strain rate sensitivity on the performance of SHCC under impact loading was previously shown in [3,4]. At higher strain rates, tensile strength and fracture energy of the matrix, tensile strength of the fiber, and fiber-matrix bond strength change as well. The unbalanced dynamic enhancement of these material parameters leads to an alteration of the micromechanical equilibrium necessary for strain-hardening and multiple cracking [1].

In M1-PE at high strain rates, the fiber-matrix bond is strongly enhanced in comparison to the weak bond observed in the quasi-static

regime, in this way also enhancing the crack-bridging capacity of the fibers.
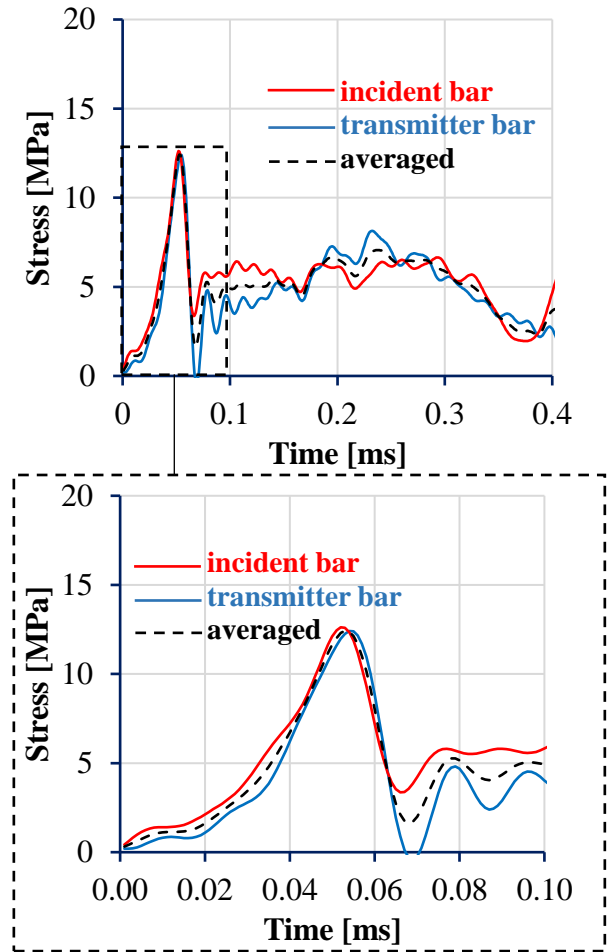
Figure 4. Stress-time histories in a M1-PE sample recorded in the input bar and transmitter bar (brass).
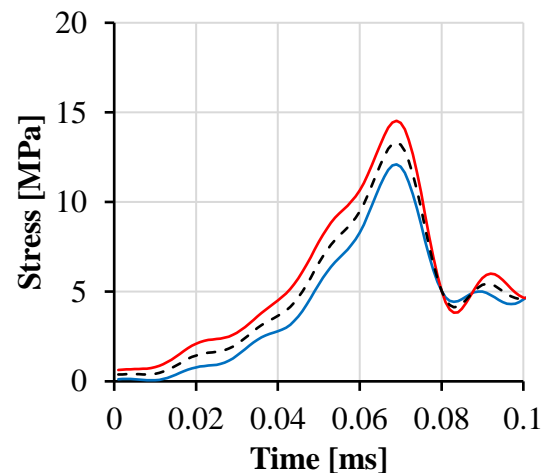
Figure 5. Stress-time history at two ends of a M1-PE sample tested with an aluminum transmitter bar.

At the same time, the dynamic increase of the tensile strength in the matrix is mainly initiated before the first crack formation. After crack formation the effective strain rate in the matrix decreases, allowing further multiple cracking due to fiber bridging at lower stress levels. The pronounced enhancement of the crack-bridging strength in combination with merely a moderate dynamic increase of the matrix's tensile strength in the cracked specimens leads to a higher number of flaws which can be activated to initiate cracks in the composite. Thus, an increase in multiple cracking is observed which results in an enhanced strain and energy absorption capacity compared to the quasi-static case.
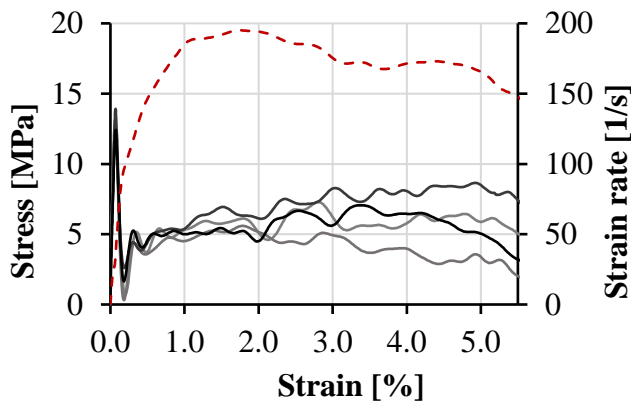
Figure 6. Stress-strain diagrams of M1-PE tested in SHTB: solid curves show stress-strain relation and red dashed curve shows the strain rate-strain relation.

Table 3. Mechanical properties of M1-PE obtained in tensile impact tests; standard deviations are given in parentheses.

First-crack stress [MPa]	13.1 (0.6)
Tensile strength [MPa]	7.1 (1.1)
Ultimate strain [%]	3.4 (1.1)
Work-to-fracture (up to softening) [kJ/m^3]	137.9 (31.3)
Young's modulus [GPa]	32.5 (8.6)

5 CONCLUSIONS

A simple, easy-to-build, gravity-driven tensile split-Hopkinson bar was designed under consideration of the challenges in testing the specific mechanical behavior of strain-hardening cement-based composites. By ensuring a sufficiently long rise time of the

input pulse and using brass with higher impedance for the transmitter bar, a uniform stress state in the samples was reached before damage initiation and formation of macro-cracks in the cement-based matrix. The loading principle based on rigid body movement of the impact flange not only increased the rise time of the input wave but also enabled to produce a sufficiently long input wave, which provided the displacement needed to cause failure in the relatively long and ductile SHCC samples. This input wave has an amplitude which results in a strain rate in the impact range. The setup can be further tuned by reducing the unsteadiness of the input wave plateau using of proper pulse shapers.

Using the setup as developed, the mechanical performance of SHCC made with a normal-strength matrix and UHMWPE fibers was studied under dynamic tensile loading. The SHCC was also tested quasi-statically for comparison. Results showed the importance of considering the strain rate sensitivity of the fiber-matrix bond when designing impact resistant SHCC. In the SHCC under investigation a weak bond exists between fibers and the matrix under quasi-static conditions, leading to mediocre mechanical performance of the composite. However, by increasing the strain rate, the change in the fiber-matrix bond resulted in better properties in terms of both strain capacity and work-to-fracture which could be traced back to the enhanced multiple-cracking behavior.

REFERENCES

[1]   V.C. Li, On engineered cementitious composites (ECC) a review of the material and its applications, J. Adv. Concr. Technol. 1 (2003) 215–230.

[2]   V. Mechtcherine, Novel cement-based composites for the strengthening and repair of concrete structures, Constr. Build. Mater. 41 (2013) 365–373.

[3]   I. Curosu, V. Mechtcherine, O. Millon, Effect of fiber properties and matrix composition on the tensile behavior of strain-hardening cement-based composites (SHCCs) subject to impact

loading, Cem. Concr. Res. 82 (2016) 23–35.

[4] I. Curosu, V. Mechtcherine, D. Forni, E. Cadoni, Performance of various strain-hardening cement-based composites (SHCC) subject to uniaxial impact tensile loading, Cem. Concr. Res. 102 (2017) 16–28.

[5] V. Mechtcherine, F.D.A. Silva, M. Butler, D. Zhu, B. Mobasher, S.-L. Gao, E. Mäder, Behaviour of Strain-Hardening Cement-Based Composites Under High Strain Rates, J. Adv. Concr. Technol. 9 (2011) 51–62.

[6] J. Harding, E. Wood, J.D. Campbell, Tensile testing of materials at impact rates of strain, J. Mech. Eng. Sci. 2 (1960) 88–96.

[7] T. Nicholas, Tensile testing of materials at high rates of strain, Exp. Mech. 21 (1981) 177–185.

[8] H. Kolsky, An Investigation of the Mechanical Properties of Materials at very High Rates of Loading, Proc. Phys. Soc. Sect. B. 62 (1949) 676.

[9] R. Gerlach, C. Kettenbeil, N. Petrinic, A new split Hopkinson tensile bar design, Int. J. Impact Eng. 50 (2012) 63–67.

[10] E. Cadoni, A. Meda, G.A. Plizzari, Tensile behaviour of FRC under high strain-rate, Mater. Struct. 42 (2009) 1283–1294.

[11] A. Chatterjee, A.L. Ruina, Two Interpretations of Rigidity in Rigid-Body Collisions, J. Appl. Mech. 65 (1998) 894.

[12] T. Gong, A.A. Heravi, I. Curosu, V. Mechtcherine, Effect of textile reinforcement on the tensile behavior of strain-hardening cement-based composites (SHCC) under quasi-static and impact loading, in: 5th Int. Conf. Prot. Struct., 2018.

[13] B. Song, W. Chen, Dynamic stress equilibration in split Hopkinson pressure bar tests on soft materials, Exp. Mech. 44 (2004) 300–312.

[14] R. Guruswami, G. Subhash, Critical Appraisal of Limiting Strain Rates for Compression Testing of Ceramics in a Split Hopkinson Pressure Bar, J. Am. Ceram. Soc. 77 (1994) 263–267.

[15] D.J. Frew, M.J. Forrestal, W. Chen, A split hopkinson pressure bar technique to determine compressive stress-strain data for rock materials, Exp. Mech. 41 (2001) 40–46.

[16] I. Curosu, M. Liebscher, V. Mechtcherine, C. Bellmann, S. Michel, Tensile behavior of high-strength strain-hardening cement-based composites (HS-SHCC) made with high-performance polyethylene, aramid and PBO fibers, Cem. Concr. Res. 98 (2017) 71–81.

[17] U. Häussler-combe, E. Panteki, Modeling of concrete spallation with damaged viscoelasticity and retarded damage, Int. J. Solids Struct. 90 (2016) 153–166.

[18] Y. Hao, H. Hao, X.H. Zhang, Numerical analysis of concrete material properties at high strain rate under direct tension, Int. J. Impact Eng. 39 (2012) 51–62.